Robust-Adaptive Finite-Time Sliding Mode Control for Flexible Joint Manipulators Facing Unknown Unbounded Disturbances

Saedeh Tavoosi[1] , Mehdi Siahi[1]*, Mohammad Reza Soltanpour[2], Ali Moarefianpour[1]

[1]Department of Mechanical, Electrical and Computer Engineering, Science and Research Branch, Islamic Azad University, Tehran, Iran, mehdi.siahi@srbiau.ac.ir
[2]Department of Electrical Engineering, Shahid Sattari Aeronautical University of Science and Technology, Tehran, Iran, soltanpour@ssau.ac.ir

Abstract

This paper addresses the stabilization of flexible joint manipulators (FJMs) under the influence of unknown and unbounded faults, model uncertainties, and external disturbances. To achieve this, the upper bound of model uncertainties and external disturbances is treated as a nonlinear function of the system states with unknown parameters. A novel robust-adaptive finite-time sliding mode controller (RAFSMC) is designed, where the unknown coefficients of the functional upper bound of disturbances are estimated using stable adaptive laws. The RAFSMC enhances the convergence speed of the flexible joints to their desired values, offering a more practical solution for the finite-time control of FJMs, even in scenarios where disturbances may have unbounded amplitudes. Initially, the equations governing the FJM model are segmented into two subsystems, after which the innovative robust-adaptive sliding mode controller is formulated, featuring a third-order finite-time sliding mode surface, a continuous control approach, and stable adaptive laws. The finite-time convergence of the FJM system states to the sliding surface is established, and a new approximation for the sign function is introduced to further reduce chattering. Stability proofs are provided using finite-time Lyapunov theory, and the simulation results, along with comparative analyses presented at the conclusion of the paper, demonstrate the effectiveness of the proposed methodology.

Keywords: Robot Manipulator, Joint Flexibility, Adaptive Sliding Mode Control, Finite-Time Control, Modeling Uncertainties, External Disturbance, Disturbance Upper Bound
Article history: Received 2024/10/31,Revised 2024/12/29; Accepted 2025/01/24, Article Type: Research paper

https://doi.org/10.82234/ijsee.2024.1189038

1. Introduction

Robotic manipulators find broad applications across a wide range of industries, such as manufacturing, sorting systems, quadruped robotics, and rehabilitation exoskeletons [1-3]. Recently, trajectory-tracking control has garnered considerable attention from the research community. Proportional-integral-derivative (PID) control is often employed due to its practical simplicity [4]. However, PID control falls short of achieving the desired performance for dynamic systems when high-performance demands or varying operating conditions are present. The design of high-performance trajectory-tracking controllers for robotic manipulators is challenging, given their nonlinear and highly coupled dynamics [5]. Moreover, nonlinear friction, parameter variations, unmodeled dynamics, payload fluctuations, and external disturbances further complicate control performance [6]. As such, advanced control schemes that are robust against disturbances are essential to meet performance goals under different conditions.

In recent decades, flexible-joint manipulators (FJMs) have gained significant popularity in human-robot interactions because of their flexibility, which enhances safety for humans [7-8]. However, FJMs are underactuated, high-order nonlinear systems, leading to complex control challenges since their order is double that of rigid manipulators and they possess fewer actuators than the number of degrees of freedom to be controlled [9]. Furthermore, FJM systems encounter uncertainties and disturbances from both the actuators and links, including variations in the environment, couplings, and

uncertainties in parameters [10-11]. This study aims to develop a precise tracking control strategy for FJMs, addressing these constraints, including unbounded perturbations.

The rapid advances in integrated circuits and computing technologies have enabled the implementation of sophisticated control strategies to improve the performance of mechatronic systems like FJMs. In [8], the authors review techniques related to flexible robotic manipulator (FRM) systems, emphasizing recent advancements in motion planning and control strategies. This work provides a comprehensive categorization of emerging research trends and applications in this field Numerous nonlinear control techniques, including backstepping [12], adaptive control [13], neural networks [14], singular perturbation control [15], and fuzzy control [16], have been applied to FJM systems. In [7], a radial basis function (RBF) neural network-based PID tuning method is proposed to enhance trajectory tracking in robotic manipulators. This method addresses uncertainties in the system dynamics by adapting the PID gains in real-time, validated through simulations with a 5-DOF manipulator. In [10], a nonlinear observer-based visual servoing approach is introduced for the vibration control of flexible manipulators using only image feedback. The method employs state estimators to regulate image positions and suppress vibrations, demonstrating its efficacy through experimental results.

Among these, sliding mode control (SMC) has gained substantial attention due to its inherent robustness against model errors, parameter uncertainties, and external disturbances [17-18]. SMC is recognized for its effectiveness in regulating robotic manipulators, offering low sensitivity to both structured and unstructured uncertainties and external disturbances. The flexibility of SMC has made it increasingly popular in recent years for controlling systems with flexible structures [19-21].

However, the main challenge with conventional SMC is the chattering effect caused by switching elements. Several methods, such as high-order SMC, boundary layer-based SMC, and observer-based SMC, have been proposed to mitigate chattering in FJM systems [22-24]. Although boundary layer-based SMC reduces chattering by using a saturation function, this approach is only effective outside the boundary layer, leading to steady-state tracking errors. Meanwhile, observer-based SMC reduces chattering by adjusting the switching gain but requires an additional observer. High-order SMC addresses continuity by incorporating higher derivatives into the control law [21].

Another issue with traditional SMC is its limited ability to handle unmatched perturbations that enter the system through various channels [25]. To address this, adaptive SMC methods have been introduced, such as the approach in [26], which addresses mismatched disturbances through a backstepping-like design. Other methods, such as the cascaded SMC scheme in [27], handle mismatched disturbances in FJM systems. While these approaches reduce the impact of such perturbations, there remains room for performance improvement due to discontinuous control laws, passive disturbance handling, or computational complexity.

Recent research has explored fractional-order SMC for FJM systems, using fractional calculus to enhance control performance [28]. Although advancements in control strategies for flexible manipulator systems have been made, handling uncertainties, disturbances, and faults remains a core research focus. Obtaining full state information from FJM systems is often costly and complex due to structural limitations, leading to the development of observer designs for these systems. For example, an extended state observer (ESO) was introduced in [11] to estimate states and uncertainties for trajectory tracking. Additionally, disturbance observers (DO) have been used to decouple joint interactions in flexible-link systems [29].

In [30], full-state feedback was employed to address trajectory tracking with variable elasticity in FJMs, ensuring the tracking error remained minimal. Other studies, such as [16], used fuzzy sliding surfaces to improve control performance, but finite-time convergence was not analyzed. While many SMC methods ensure asymptotic stability, finite-time stability offers more precise control within a specified time frame. Neural networks and Kalman filters were used in [23] to address chattering, but finite-time convergence was not discussed. In contrast, the method proposed here offers a comprehensive finite-time control solution that extends beyond chattering reduction. While research in [12, 31-33] emphasizes robustness, finite-time convergence is not covered. A terminal sliding mode control (TSMC) approach with a cascaded finite-time sliding mode observer (CFTSMO) was proposed in [34] for robust finite-time convergence and disturbance attenuation. Additionally, a nonsingular fast terminal sliding mode controller (NFTSMC) with a finite-time extended state observer (FTESO) was designed for trajectory tracking in FJMs [35]. A recent study in [36] introduced a super-twisting adaptive SMC, addressing input saturation constraints and claiming finite-time stability. In [37], a nonlinear I-PID-type control scheme is presented for torque-driven flexible joint robots facing input saturation. The proposed controller ensures global asymptotic stability in the presence of disturbances and uncertainties, validated by real-time experiments on a two-degrees-of-freedom manipulator.

Recently in [38], a nonsingular fixed-time sliding mode controller is proposed to mitigate the effects of friction, dynamic parameter uncertainty, and external disturbances in flexible manipulators. By incorporating a generalized disturbance estimator and adaptive RBF neural networks, the approach demonstrates substantial improvements in control accuracy. In [39], an adaptive integral sliding mode controller (AISMC) based on singular perturbation theory is developed for flexible joint robots. This controller effectively reduces tracking errors and noise, proving its stability and robustness through experimental validation. Finally, in [40], a method for designing an adaptive sliding mode control law for flexible joint manipulators is presented. The proposed controller aims to counter disturbances affecting the actuator signals, with its stability verified by the Lyapunov method and performance assessed through simulations and real-time responses.

In practical applications, FJM systems encounter unmodeled dynamics and external factors like wind or unwanted forces, which are modeled as external disturbances. Unlike earlier studies, where disturbances were considered independent variables, this work recognizes that disturbances and uncertainties depend on system states, such as the position and orientation of the FJM end-effector. This means the upper bound of disturbances and uncertainties is not necessarily a scalar value but a nonlinear function of system states. Moreover, the coefficients of this nonlinear function are unknown and need to be estimated through adaptive rules, making the control problem more realistic.

This study presents a novel robust-adaptive finite-time sliding mode controller (RAFSMC) designed to stabilize FJM systems, where the upper bound of disturbances is an unknown, nonlinear state-dependent function. The chattering phenomenon is effectively addressed by approximating the sign function in SMC, ensuring smooth control input without chattering. The key innovation of this paper lies in considering the upper bound of disturbances as a nonlinear function of system states with unknown coefficients, a significant improvement over previous SMC controllers for finite-time trajectory tracking in FJM systems.

A novel terminal robust adaptive finite-time sliding mode control (RAFSMC) for trajectory tracking of FJM robot end-effectors exposed to unknown perturbations. The continuous sliding mode surface reduces chattering while maintaining performance.

The proposed controller can handle unbounded external disturbances and uncertainties, where the upper bound is a nonlinear function of system states with unknown coefficients, estimated using adaptive laws. This is a departure from previous studies that assume a constant upper bound for disturbances.

The rest of the paper is structured as follows: Section II outlines the FJM model, problem formulation, and necessary preliminaries. Section III presents the proposed controllers, including SMC and robust-adaptive SMC. Simulation results are given in Section IV to validate the theoretical findings. The conclusion is provided in Section V.

2. Flexible joint manipulators modeling

The dynamic model of a flexible robot is represented by the following equations, with the derivation process omitted here. For detailed explanations, refer to [39].

$$D(\theta)\ddot{\theta} + C(\theta,\dot{\theta})\dot{\theta} + g(\theta) = K_s(r\theta_m - \theta) \tag{1}$$

$$J\ddot{\theta}_m + (B + R_m^{-1}K_mK_b)\dot{\theta}_m + rK_s(r\theta_m - \theta) = R_m^{-1}K_mU \tag{2}$$

where $\theta \in R^n$and $\theta_m \in R^n$ respectively denote the joint angle and rotor position vectors, $U \in R^n$ is the vector of motors voltage, $D \in R^{n\times n}$ is the manipulator inertia matrix, $C \in R^{n\times n}$ denotes the Centrifugal and Coriolis terms matrix and $g \in R^n$ is gravitation force vector. In equation (2), $J \in R^{n\times n}$, $B \in R^{n\times n}$, $r \in R^{n\times n}$ and $R_m \in R^{n\times n}$ respectively indicate the coefficients of the motor's inertia, motors damping, reduction gear and armature resistance. $K_s, K_m, K_b \in R^{n\times n}$ are some constant diagonal matrices [39].

We proceed with modeling the flexible-joint robot in the presence of faults, disturbances, and uncertainties. The mechanical dynamics of the system are captured by the dynamic equations (Eq. 1), while the electrical dynamics are described in Eq. (2), where DC motor voltages serve as the control inputs [39]. Disturbances, such as unmodeled dynamics, are considered within Eq. (1) in accordance with standard approaches from the literature. Furthermore, an input bias fault is introduced into Eq. (2), necessitating its inclusion alongside the system input term. This ensures that the input bias fault is positioned consistently with respect to the system input. Consequently, the dynamic equations, accounting for unmodeled dynamics and input faults, provide an extended version of the nominal model described in Eqs. (1) and (2).

$$D(\theta)\ddot{\theta} + C(\theta,\dot{\theta})\dot{\theta} + g(\theta) + \Delta f(\theta) = K_s(r\theta_m - \theta) + d_s \tag{3}$$

$$J\ddot{\theta}_m + (B + R_m^{-1}K_mK_b)\dot{\theta}_m + rK_s(r\theta_m - \theta) = R_m^{-1}K_mU + F_af_a + d_m \tag{4}$$

Where $f_a \in R^n$ represents the unknown actuator error, $F_a \in R^{n\times n}$ is the fault input matrix and $\Delta f \in R^n$ is a vector encompassing unknown dynamics and modelling uncertainties. Also $d_m, d_s \in R^n$ stands for external disturbances. It is

also worth to mention that due to the presence of various types of faults such as disturbances in the voltage or current in the energy supply system in the manipulator or other faults, the possibility of the fault entering the robot system from its energy source, i.e. the voltage and current of the motor, is high. For this reason, the fault is considered in the introduced robot model as the input bias

A) Rewriting the robot model with flexible joints in nonlinear state space form

The flexible robotic arm model outlined in Eqs. (3) and (4) possesses 4n degrees of freedom. In this section, we will apply a transformation to express these equations in a more standard nonlinear state-space format. This transformation simplifies the application of established theorems for designing stabilizing control strategies. The transformation of the variables is defined as follows:

$$x_1 = \theta, x_2 = \theta_m \quad (5)$$

$$x_3 = \dot{\theta}, x_4 = \dot{\theta}_m$$

The model of the mechanical arm with flexible joints, incorporating faults and unmodeled dynamics as detailed in Eqs. (3) and (4), can be expressed as follows:

$$\dot{x}_1 = x_3 \quad (6)$$

$$\dot{x}_2 = x_4$$

$$\dot{x}_3 = D^{-1}(x_1)\{K_s(rx_2 - x_1) - C(x_1, x_3)x_3 - g(x_1) - \Delta f(x) + d_s\}$$

$$\dot{x}_4 = J^{-1}\{R_m^{-1}K_m U + F_a f_a + d_m - (B + R_m^{-1}K_m K_b)x_4 - rK_s(rx_2 - x_1)\};$$

where $x_i \in R^n$ for $i = 1,2,\dots,4$. By defining $x = [x_1, x_2, x_3, x_4]^T \in R^{4n}$,
Eq. (6) can alternatively be represented in the following more consolidated form:

$$\dot{x} = Ax + BU + H + \Phi \quad (7)$$

where

$$A = \begin{bmatrix} 0 & 0 & 1 & 0 \\ 0 & 0 & 0 & 1 \\ 0 & 0 & 0 & 0 \\ J^{-1}rK_s & -J^{-1}rK_s r & 0 & -J^{-1}(B + R_m^{-1}K_m K_b) \end{bmatrix} \in R^{4n\times 4n}; \quad B = \begin{bmatrix} 0 \\ 0 \\ 0 \\ J^{-1}R_m^{-1}K_m \end{bmatrix} \in R^{4n\times n}; \quad (8)$$

$$H(x,t) = \begin{bmatrix} 0 \\ 0 \\ -D^{-1}(x_1)(\Delta f(x) + d_s) \\ J^{-1}(F_a f_a + d_m) \end{bmatrix} \in R^{4n}; \ \Phi(x,t) = \begin{bmatrix} 0 \\ 0 \\ D^{-1}(x_1)\{K_s(rx_2 - x_1) - C(x_1, x_3)x_3 - g(x_1)\} \\ 0 \end{bmatrix} \in R^{4n}$$

Following the definition of the error, tracking the desired configuration in the dynamic model of the flexible-joint robot is defined as follows:

$$\hat{x} = x - x_{des} \in R^{4n} \quad (9)$$

where $x_{des} = [\theta_{des}, \theta_{m\,des}, \dot{\theta}_{des}, \dot{\theta}_{m\,des}]^T \in R^{4n}$ we can reformulate the dynamic model of the configuration error using the state-space dynamic model from (7) as follows:

$$\dot{\hat{x}} = \dot{x} - \dot{x}_{des} = Ax + BU + H(x,t) + \Phi(x,t) - \dot{x}_{des} \quad (10)$$

By substituting x with $x = \hat{x} + x_{des}$ from Eq. (9) into Eq. (10), we obtain:

$$\dot{\hat{x}} = A\hat{x} + BU + H(x,t) + Ax_{des} + \Phi(x,t) - \dot{x}_{des} \quad (11)$$

Finally, we propose a nonlinear error model for the generalized robot model with flexible joints, expressed as follows:

$$\dot{\hat{x}} = A\hat{x} + BU + H(x,t) + \widehat{\Phi}(x,t) \quad (12)$$

where $\widehat{\Phi} \in R^{4n}$ is a known vector defined as follows:

$$\widehat{\Phi}(x,t) = Ax_{des} + \Phi(x,t) - \dot{x}_{des} \quad (13)$$

B) Problem formulation and preliminaries

In practical applications, the dynamic model of a flexible-joint manipulator (FJM) is subject to external disturbances, uncertainties in model parameters, and unmodeled dynamics. The dynamic parameters of an FJM system, such as inertia, mass, friction, and parameters related to the motors including motor inertia, damping, gear reduction, and armature resistance are often treated as uncertain by designers.

Additionally, FJMs frequently encounter external disturbances like wind or other unknown forces, as well as undesirable fluctuations in the input voltage to the FJM motors. To address these challenges, the following remark provides a more accurate and applicable description of the FJM system:

Remark 1: The model uncertainty $\Delta f(x)$ is dependent on the states of the FJM system. Furthermore, external disturbances are also influenced by the end-effector position of the FJM robot. Thus, for the first time, this study posits that the upper bound of external disturbances and model uncertainties, denoted as $H(\hat{x}, t)$, is not merely a scalar value but a nonlinear function of the FJM state variables. Moreover, it is assumed that the coefficients of this upper bound function are unknown, and stable adaptive laws will be developed to estimate these coefficients. This leads to more realistic and applicable assumptions regarding the FJM trajectory tracking problem. Therefore, consider the following applicable assumption:

Assumption 1: Assume that the upper bound of the vector of model uncertainties and external disturbances in the FJM model, as indicated in (12), is constrained as follows:

$$\|H(x(t),t)\| \le \alpha h(x(t),t) + \beta \quad (14)$$

in which α and β refer to the unknown values and $h(x(t),t)$ refers to an arbitrary nonlinear function of the FJM system state variables.

Remark 2: Using assumption 1, the only constraint on the type and shape of uncertainties and disturbances is that they must have functional upper bounds that are nonlinear functions of the system states. However, while the disturbances are allowed to grow unbounded in magnitude, their growth rate must not exceed the capacity of the adaptive laws to estimate and compensate for them. The disturbance functions are generally assumed to be smooth (e.g., Lipschitz continuous or continuously differentiable). This ensures that the adaptive estimation and control laws remain stable. Completely arbitrary, highly oscillatory, or stochastic disturbances that do not fit within a structured bound framework may not be effectively attenuated by this method.

This paper aims to develop Robust Adaptive Finite-Time Sliding Mode Control (RAFSMC) laws for the nonlinear flexible-joint manipulator (FJM) system, which encounters external disturbances and model uncertainties as described in (12). By considering Assumption 1 and designing the proposed controllers, the convergence of $\hat{x} = x - x_{des}$ to zero within a predefined finite time will be achieved. Additionally, adaptive rules are formulated to estimate the functional upper bound coefficients of the external disturbances and model uncertainties indicated in (14).

In contrast to previous research, we introduce two key assumptions in this article: firstly, we do not possess knowledge of the actual values of uncertainties and disturbances, nor their upper bounds; secondly, convergence occurs in a predefined finite time, rather than asymptotically, as seen in other studies that theoretically suggest convergence in an infinite and unknown timeframe. These assumptions enhance the practicality of addressing the stabilization problem for the FJM system under more realistic conditions.

Before we proceed with the design of the finite-time adaptive robust sliding mode control law in the following section, we will present the two lemmas:

Lemma 1 [41]: Suppose there exists a Lyapunov function with initial conditions such that:

$$\dot{V}(x) + \alpha V(x) + \beta V^{\gamma}(x) \le 0 \quad (15)$$

in which $\alpha, \beta > 0$ and $0 < \gamma < 1$. Then this Lyapunov function tends to zero in finite time with the following settling time:

$$T \le \alpha^{-1}(1-\gamma)^{-1} ln(1 + \alpha\beta^{-1}V_0^{1-\gamma}) \quad (16)$$

Lemma 2 [42]: in the following non-linear differential equation:

$$\dot{x} + \lambda sig(x)^{\beta} = 0 \quad (17)$$

where $x \in \mathcal{R}^n$, $\lambda = diag(\lambda_i)$ is a positive definite matrix with elements $\lambda_i \in \mathcal{R}^+$for $i = 1,2,...,n$ and $sig(x)^{\beta} = [|x_1|^{\beta} sign(x_1), \dots, |x_n|^{\beta} sign(x_n)]^T$and $0 < \beta < 1$. The state vector of the system i.e. $x \in \mathcal{R}^n$converges to zero in the finite time $T = \max(T_i), i = 1, \dots, n$ where we have:

$$T_i = \frac{1}{\lambda(1-\beta)} |x_{0i}|^{1-\beta} \quad (18)$$

3. Robust-adaptive finite time sliding mode controller design

In this section, we present a sliding mode control law aimed at achieving the specified configuration for the flexible robot, as defined in (12). The primary objective of this control law is to guide the flexible-joint robot to the desired configuration within a finite timeframe. To facilitate system stabilization, we employ the adaptive terminal sliding mode control rule in the controller design. This approach involves first creating a stable finite-time sliding surface, followed by the application of the control rule to reach this sliding surface, ultimately ensuring the stabilization of the system within a finite time.

It should be noted that the process of designing the adaptive robust sliding mode control law meaning RAFSMC design procedure in this paper is carried out step by step in the following:

- Sliding surface design: Selecting a finite time sliding surface consists of a stability equation for tracking error (Subsection A)
- Finite time stability of error in sliding mode: Prove that with this sliding surface, the tracking error becomes zero in finite time in sliding mode of system and also finding this finite time (Lemma 3).
- RAFSMC controller design: By setting the reaching law in sliding mode concept equal to the derivative of the sliding surface (Subsection B).
- RAFSMC Stability Proof: Choosing a Lyapunov function and showing that by applying the final designed control rule and adaptive rules, the derivative of the Lyapunov function will be negative (Theorem 1).
- Adaptive rules design: Adaptive rules are also designed to help make the derivative of the Lyapunov function negative (Proof of Theorem 1)
- Finite Time Stability of sliding surface: Showing the system to transition from the initial

conditions to the sliding surface (enter the sliding mode) in finite time. Choosing another Lyapunov function consists of only the sliding surface norm.

- Chattering reduction: Presenting a new method for improvement of Discontinuity (Chattering) in the Controller by modifying the sign function (Subsection C)

A) Finite Time Sliding Surface Design

Given the error model in (12), we define the following sliding surface:

$$s(t) = C\hat{x}(t) + kC\int(\hat{x}(t) + sig(\hat{x})^{\gamma}) \quad (19)$$

where $C \in R^{2n\times 4n}$ is a design parameter matrix, chosen based on the subsequent excitation and determined later. The vector $s(t) \triangleq [s_1, s_2, \dots, s_{2n}] \in R^{2n}$ represents the sliding surface, $k \in R^{+}$ is a constant positive real number, $\gamma \in (0,1)$and $sig(\hat{x})^{\gamma}$ are defined as

$$sig(\hat{x})^{\gamma} = [|\hat{x}_1|^{\gamma}sign(\hat{x}_1), \dots, |\hat{x}_{4n}|^{\gamma}sign(\hat{x}_{4n})]^T \quad (20)$$

In accordance with the principles of sliding mode control, both the sliding surface and its derivative must be set to zero. Thus, it is essential to satisfy the following conditions

$$s(t) = 0\ , \dot{s}(t) = 0 \quad (21)$$

By combining the two aforementioned relationships, the dynamics of the system in the sliding mode can be expressed as:

$$C\dot{\hat{x}}(t) + kC(\hat{x}(t) + sig(\hat{x})^{\gamma}) = 0, \quad (22)$$

Hence, it follows:

$$\dot{\hat{x}}(t) = -k(\hat{x}(t) + sig(\hat{x})^{\gamma}) \quad (23)$$

In the subsequent analysis, we first establish the finite-time stability of the sliding surface (19). Specifically, we will demonstrate that in the sliding mode of the flexible-joint robot system, once the system reaches the sliding plane, it achieves asymptotic stability, with the value converging to zero within a finite time. In essence, $\hat{x}(t)$ will achieve convergence within a defined duration.

To begin, consider the following lemma:

Lemma 3: The sliding mode dynamics described in (23) exhibit asymptotic stability, and $\hat{x}(t)$ converges to the equilibrium point $\hat{x}(t)$ =0 within a finite time.

Proof:

We consider the subsequent candidate Lyapunov function:

$$V(t) = \|\hat{x}(t)\| \quad (24)$$

The derivative of this function along the trajectory of the system (23) is:

$$\dot{V}(t) = sign(\hat{x})^T\dot{\hat{x}} = sign(\hat{x})^T(-k(\hat{x}(t) + sig(\hat{x})^{\gamma})) \quad (25)$$
$$= -k(sign(\hat{x})^T\hat{x} + sign(\hat{x})^T sign(\hat{x})^{\gamma})$$
$$= -k(\|\hat{x}\| + \|\hat{x}\|^{\gamma})$$

Owing to the positive terms$\|\hat{x}\|$ and $\|\hat{x}\|^{\gamma}$, it can be straightforwardly expressed as:

$$\dot{V}(t) \le -k\|\hat{x}\| \quad (26)$$

Up to this point, we have established the asymptotic stability of $\hat{x}$ toward zero. Now, we will examine its finite-time convergence. By utilizing (25), we can derive:

$$\dot{V}(t) = \frac{d\|\hat{x}\|}{dt} = -k(\|\hat{x}\| + \|\hat{x}\|^{\gamma}), \quad (27)$$

and we continue:

$$dt = -\frac{d\|\hat{x}\|}{k(\|\hat{x}\| + \|\hat{x}\|^{\gamma})} = -\frac{\|\hat{x}\|^{-\gamma}d\|\hat{x}\|}{k(\|\hat{x}\|^{1-\gamma} + 1)} \quad (28)$$
$$= -\frac{d\|\hat{x}\|^{1-\gamma}}{k(1-\gamma)(\|\hat{x}\|^{1-\gamma} + 1)}$$

By integrating both sides of Eq. (28) from time t_1 (the moment when the state $\hat{x}$ reaches the sliding surface $s(t) = 0$) to the time t_2 (when $\hat{x}$ converges to zero) and considering $\hat{x}(t_2)$, we can readily deduce:

$$t_2 - t_1 = -\frac{1}{k(1-\gamma)}\int_{\hat{x}(t_1)}^{\hat{x}(t_2)}\frac{d\|\hat{x}\|^{1-\gamma}}{(\|\hat{x}\|^{1-\gamma} + 1)} \quad (29)$$
$$= -\frac{1}{k(1-\gamma)}ln(\|\hat{x}\|^{1-\gamma} + 1)\Big|_{\hat{x}(t_1)}^{\hat{x}(t_2)}$$
$$= -\frac{1}{k(1-\gamma)}(ln(\|\hat{x}(t_2)\|^{1-\gamma} + 1) - ln(\|\hat{x}(t_1)\|^{1-\gamma} + 1))$$
$$= \frac{1}{k(1-\gamma)}ln(\|\hat{x}(t_1)\|^{1-\gamma} + 1)$$

Consequently, the trajectory of the state $\hat{x}$ from the instant of reaching the sliding surface converges to zero within the finite time t_2:

$$t_2 = t_1 + \frac{1}{k(1-\gamma)}ln(\|\hat{x}(t_1)\|^{1-\gamma} + 1) \quad (30)$$

And this end the proof.

Remark 3: It is crucial to note that the value of $\hat{x}$ converges to zero within the finite time as per Eq. (30). According to Lemma 3, this implies that reaching the sliding surface at time t_1, results in the convergence to the desired configuration and the reduction of the tracking error to zero within the limited time t_2 expressed in Eq. (30).

B) Design of the Robust Adaptive Finite-time Sliding Mode Controller (RAFSMC)

To design the RAFSMC controller, we first derive the derivative of the sliding surface as defined in equation (19):

$$\dot{s}(t) = C\dot{\hat{x}}(t) + kC(\hat{x}(t) + sig(\hat{x}(t))^{\gamma}) \quad (31)$$

By substituting the FJM system from equation (12) into (31), we have:

$$\dot{s}(t) = C\{A\hat{x} + BU + H(x,t) + \hat{\Phi}(x,t)\} + kC(\hat{x}(t) + sig(\hat{x}(t))^{\gamma}) \quad (32)$$

We now propose the finite-time adaptive sliding mode control law, formulated as follows:

$$\begin{aligned} U(t) = (CB)^{-1}\{&-\mu s \\ &-\left(\rho + \|C\|\hat{\beta} + \|C\|\hat{\alpha}h(x(t),t)\right)sgn(s) \\ &-C\hat{\Phi} - kC(\hat{x}(t) + sig(\hat{x}(t))^{\gamma}) \\ &- CA\hat{x}\} \end{aligned} \quad (33)$$

where the values of $\hat{\beta}$ and $\hat{\alpha}$ are estimating and obtaining from the following adaptive laws:

$$\begin{aligned} \dot{\hat{\alpha}}(t) &= k_1\|C\|s^T\, sgn(s)h(x(t),t) \\ \dot{\hat{\beta}}(t) &= k_2\|C\|s^T\, sgn(s) \end{aligned} \quad (34)$$

where $k_1, k_2 > 0$ are two positive values which known as adaptive gains. The conclusion reached in this section is presented in the following theorem.

Theorem 1: Consider the flexible-joint manipulator (FJM) model outlined in (12), which is subjected to faults, modeling uncertainties, and external disturbances, along with Assumption 1. By implementing the control law (33) in conjunction with the adaptation laws (34), if the constants k, ρ ، β and μ are selected such that $\rho > 0$, $k > 0$ and $\mu, \lambda > 0$, $0 < \beta < 1$ the flexible robot manipulator system will achieve stabilization, and the system states, including the robot joints, will converge to the desired values within a finite time.

Proof: To establish stability, we initially choose the Lyapunov function as follows:

$$V = \frac{1}{2}s(t)^T s(t) + \frac{1}{2k_1}\tilde{\alpha}(t)^2 + \frac{1}{2k_2}\tilde{\beta}(t)^2 \quad (35)$$

where $k > 0$ and $\tilde{\alpha}(t) = \hat{\alpha}(t) - \alpha$ and $\tilde{\beta}(t) = \hat{\beta}(t) - \beta$ are the errors between the true values and estimations of the perturbation's functional upper bounds. Then by derivation of (35) with respect to time and substituting from (32) we have, given that $\dot{\tilde{\alpha}} = \dot{\hat{\alpha}}$ and $\dot{\tilde{\beta}} = \dot{\hat{\beta}}$, results in

$$\begin{aligned} \dot{V} &= s(t)^T\dot{s}(t) + \frac{1}{k_1}\tilde{\alpha}\dot{\hat{\alpha}} + \frac{1}{k_2}\tilde{\beta}\dot{\hat{\beta}} \\ &= s(t)^T\{C\{A\hat{x} + BU + H(x,t) + \hat{\Phi}(x,t)\} \\ &\quad + kC(\hat{x}(t) + sig(\hat{x}(t))^{\gamma}) \\ &\quad + \frac{1}{k_1}(\hat{\alpha}(t) - \alpha)\dot{\hat{\alpha}} + \frac{1}{k_2}(\hat{\beta}(t) \\ &\quad - \beta)\dot{\hat{\beta}} \end{aligned}$$

Next, by replacing the designed controller in (33) and the adaptive laws (34) into (36), we have:

$$\begin{aligned} \dot{V} &= s^T\Big(-\mu s \\ &\quad -\left(\rho + \|C\|\hat{\beta} + \|C\|\hat{\alpha}h(x(t),t)\right)sgn(s) \\ &\quad + CH(x,t)\Big) \\ &\quad + (\hat{\alpha}(t) - \alpha)\|C\|s^T\, sgn(s)h(x(t),t) \\ &\quad + \left(\hat{\beta}(t) - \beta\right)\|C\|s^T\, sgn(s) \\ &= -\mu\|s\|^2 - \rho\|s\| - \|C\|\hat{\beta}\|s\| \\ &\quad - \|C\|\hat{\alpha}h(x(t),t)\|s\| \\ &\quad + s^T CH(x,t) \\ &\quad + \hat{\alpha}\|C\|\|s\|h(x(t),t) \\ &\quad - \alpha\|C\|\|s\|h(x(t),t) \\ &\quad + \hat{\beta}(t)\|C\|\|s\| \\ &\quad - \beta\|C\|\|s\| \end{aligned} \quad (36)$$

where removing the similar terms simplifies (37) as follows

$$\begin{aligned} \dot{V} = -\mu\|s\|^2 - \rho\|s\| + s^T CH(\hat{x},t) \\ - \alpha\|C\|\|s\|h(x(t),t) \\ - \beta\|C\|\|s\| \end{aligned} \quad (37)$$

On the other hand, by using equation (14) in Assumption 1, it can be written:

$$\begin{aligned} s^T CH(\hat{x},t) &\le \|s\|\|C\|\|H(\hat{x},t)\| \\ &\le \|s\|\|C\|(\alpha h(x(t),t) \\ &\quad + \beta) \\ &= \|C\|\|s\|\alpha h(x(t),t) \\ &\quad + \|C\|\|s\|\beta \end{aligned} \quad (38)$$

By merging equations (37) and (38), the upper bound of the derivative of the Lyapunov function is obtained as follows:

$$\dot{V} \le -\mu\|s\|^2 - \rho\|s\| \le 0 \quad (39)$$

Consequently, under the conditions $\mu, \rho > 0$, the derivative of the Lyapunov function becomes negative. Therefore, since the Lyapunov function is positive definite and its time derivative is negative, we can conclude, in accordance with the Lyapunov stability theorem and Barbalat's lemma, that the value of the sliding surface $s(t)$ tends to zero. As $s(t)$approaches zero, based on equation (23) and Lemma 3, we can conclude that $\hat{x}(t) = 0$. Consequently, within the finite time specified in Lemma 3, the convergence of $x \to x_{des}$ is achieved, which we denote as T_e.

However, the proof does not conclude here. We must now demonstrate that by employing the control laws (33) and (34), the system itself also reaches the sliding surface within a finite time, which we refer to as T_s (the time taken for the system to transition from the initial conditions to the sliding surface and enter the sliding mode). As a result, we can conclude that the total error $\hat{x}$ converges to zero within a finite time, $T_{final} = T_s + T_e$. For this purpose, we will consider the following new Lyapunov

$$V_s = \frac{1}{2}s^T s \quad (40)$$

Differentiating from (40) and substituting from (32) and then (33) we have

$$\begin{aligned}\dot{V}_s &= s(t)^T \dot{s}(t)\\ &= s(t)^T \Big(-\mu s\\ &- \Big(\rho + \|C\|\hat{\beta} + \|C\|\hat{\alpha}h(x(t),t)\Big) sgn(s)\\ &+ CH(x,t)\Big)\\ &\le -\mu\|s\|^2 - \rho\|s\| - \|C\|\hat{\beta}\|s\|\\ &- \|C\|\hat{\alpha}h(x(t),t)\|s\| + s^T CH(x,t)\end{aligned} \quad (41)$$

Using (38), we have

$$\begin{aligned}\dot{V}_s \le -\mu\|s\|^2 &- \rho\|s\| - \|C\|\hat{\beta}\|s\|\\ &- \|C\|\hat{\alpha}h(x(t),t)\|s\|\\ &+ \|C\|\|s\|\alpha h(x(t),t)\\ &+ \|C\|\|s\|\beta\end{aligned} \quad (42)$$

Now, according to the definitions $\tilde{\alpha}(t) = \hat{\alpha}(t) - \alpha$ and $\tilde{\beta}(t) = \hat{\beta}(t) - \beta$, one can write inequality in (42) as follows

$$\begin{aligned}\dot{V}_s \le -\mu\|s\|^2 &- \rho\|s\| - \tilde{\beta}\|C\|\|s\|\\ &- \|C\|\tilde{\alpha}h(x(t),t)\|s\|\end{aligned} \quad (43)$$

Now, from stability of Lyapunov function in (35) and stability of adaptive laws in (34), its easy to conclude that:

$$|\tilde{\alpha}| \le \bar{\alpha} \ , \ |\tilde{\beta}| \le \bar{\beta} \quad (44)$$

where $\bar{\alpha}$ and $\bar{\beta}$ are two finite real positive numbers. Therefore from (43) it is concluded that

$$\begin{aligned}\dot{V}_s \le -\mu\|s\|^2 &- \rho\|s\| + \bar{\beta}\,\|C\|\|s\|\\ &+ \|C\|\bar{\alpha}h(x(t),t)\|s\|\\ &= -\mu\|s\|^2 - \rho\|s\|\\ &+ \|C\|\|s\|\big(\bar{\alpha}h(x(t),t)\\ &+ \bar{\beta}\big)\end{aligned} \quad (45)$$

From boundedness of $\bar{\alpha}, \bar{\beta}$ and $h(x(t),t)$ and $\|C\|$ and considering their upper bound as $\|C\|\|\bar{\alpha}h(x(t),t) + \bar{\beta}\| \le \delta$, (45) can be expressed as follows:

$$\dot{V}_s \le -\mu\|s\|^2 - \rho\|s\| + \delta\|s\| \quad (46)$$

By defining $\rho_n = \rho - \delta$ and selecting $\rho > \delta$ and therefore $\rho_n > 0$, we can write the relation (46) as follows:

$$\dot{V}_s \le -\mu\|s\|^2 - \rho_n\|s\| \quad (47)$$

According to (40) and replacing $\|s\| = \sqrt{2V_s}$ in (47) we have:

$$\dot{V}_s \le -\mu 2V_s - \rho_n\sqrt{2}V_s^{\frac{1}{2}} \quad (48)$$

As a result, using Lemma 1 and (45), the Lyapunov function defined in (40) confirms that the sliding surface converges to zero within a finite time:

$$T_s \le (\mu)^{-1}\, ln(1 + \sqrt{2}\mu(\rho_n)^{-1}V_0^{\frac{1}{2}}) \quad (49)$$

Finally, the zeroing of the error and the convergence of $x \to x_{des}$ is achieved in the finite time $T_{final} = T_s + T_e$.■

Using T_e from equation (30) and T_s from equation (49), the finite time of convergence of robot joints to their desired values can be calculated as $T_{final} = T_s + T_e = (\mu)^{-1}\, ln(1 + \sqrt{2}\mu(\rho_n)^{-1}V_0^{\frac{1}{2}}) + \frac{1}{k(1-\gamma)} ln(\|\hat{x}(t_1)\|^{1-\gamma} + 1)$.

The Robust-Adaptive Finite-Time Sliding Mode Control (RAFSMC) which is proposed in Theorem1 for Flexible Joint Manipulators (FJMs) is designed to address a broad range of disturbances, provided they meet certain criteria.

The only constraint on model uncertainties and external disturbances in the FJM model is Assumption 1, where it is assumed that upper bound of perturbations is constraint by a nonlinear function like $\alpha h(x(t),t) + \beta$. Nevertheless, the types of disturbances and uncertainties that can be attenuated by RAFSMC, can be presented as follows:

- Unknown and Unbounded Disturbances: The controller can manage external disturbances and faults whose amplitudes may grow without bound over time. These disturbances are modeled such that their upper bounds are nonlinear functions of the system states. The parameters of these bounds are unknown but estimated adaptively by the controller.
- Model Uncertainties: The RAFSMC is robust against uncertainties in the dynamic model of the manipulator, such as parameter variations or unmodeled dynamics. It does not require precise knowledge of the uncertainties, as the adaptive mechanism compensates for their effects.
- External Disturbances: Environmental forces, payload changes, and interaction-induced vibrations are effectively handled. The disturbances must conform to the assumption that their upper bounds can be expressed as a functional relationship with system states.
- Unknown Faults: Mechanical or actuator faults are included in the class of disturbances the controller can handle, as long as their impact on the system is representable within the assumed bound framework.

C) Improvement of Discontinuity (Chattering) in the Controller

The existing discontinuity due to the presence of the sign function in the control law leads to a phenomenon known as chattering. This chattering causes high-frequency fluctuations in the input to the robot system, potentially damaging its mechanical components. To mitigate this phenomenon, it is essential to modify the sign function in u within the control law to ensure continuity and avoid discontinuities.

Several suggestions have been proposed to address this issue, such as using the hyperbolic tangent function $tan\,h(s)$ or a saturation function, denoted as $sat(s)$,. While these solutions reduce chattering, they can also diminish control efficiency due to alterations in the controller's nature.

This article introduces a novel approach to resolve this issue. Recognizing that discontinuity occurs when s converges to zero or is near zero, we propose adding a term to the control input u. Specifically, we consider the term $\rho sign(s)$ seen in the control laws and adaptive laws as follows:

$$u = \rho sign(s) \cong \frac{\rho^2 s}{\rho\|s\| + \sigma(t)} \tag{50}$$

In this relation, $\sigma(t)$ is a positive function such that $\int_0^\infty \sigma(t)dt < \infty$. This modification addresses the discontinuity issue in the control law. The choice of the function $\sigma(t)$ is arbitrary; for example, one option can be:

$$\sigma(t) = \frac{1}{1+t^n} \quad n \geq 2 \tag{51}$$

It is noteworthy that when $\sigma(t)$ approaches zero, the value of u in (50) will behave similarly to the previous state $\frac{s}{\|s\|}$

Remark 4. It is essential to clarify that the parameters are chosen based on the conditions established in Theorem 1, and during the discussion of the sliding surface and control law and also adaptive equations. The parameters must therefore satisfy the following conditions: $\rho > 0,\ k > 0,\ 0 < \gamma < 1,$ $(\mu, \lambda > 0),\ 0 < \beta < 1,\ k_1, k_2 > 0.$

While these conditions are sufficient for the control law to be applicable for achiving finite time stability in FJM, it is crucial to understand that any adjustment to these parameters will affect the system's response. For example k influences the convergence rate of $\hat{x}(t)$, as demonstrated in Equation (23). Furthermore, the finite time of convergence derived in Equations (30) and (49) and finally $T_{final} = T_s + T_e = (\mu)^{-1} ln(1 + \sqrt{2}\mu(\rho_n)^{-1}V_0^{\frac{1}{2}}) + \frac{1}{k(1-\gamma)} ln(\|\hat{x}(t_1)\|^{1-\gamma} + 1)$, is dependent on these parameters and may be tailored according to the desired convergence behavior.

4. Simulations results

In this section, the RAFSMC designed in the previous segment is demonstrated through several numerical examples. By considering disturbances, faults, and other uncertainties in the model of a flexible-joint robotic arm, we utilize the finite-time adaptive sliding mode control (SMC) to show that the established stable finite-time sliding mode control law enables effective trajectory tracking within a finite time frame.

For the sake of demonstration, a numerical example is set up to simulate the performance of the RAFSMC under various operating conditions. The flexible-joint robotic arm model is subjected to unmodeled dynamics and external disturbances, simulating real-world scenarios that a robotic system may encounter.

For the simulation, we utilize the single-RLFJ (Rotary-Linear-Flexible-Joint) robotic arm model presented in [43], incorporating its dynamic parameters. The specifications of this robot are outlined as follows [43]:

$$\begin{aligned} &(J_{eq} + J_{Arm})\ddot{\theta}_m + J_{Arm}\ddot{\alpha} \\ &\qquad - mghsin(\theta_m + \alpha) \\ &\qquad + B_{eq}\dot{\theta}_m = \tau_m \\ &J_{Arm}(\ddot{\theta}_m + \ddot{\alpha}) - mghsin(\theta_m + \alpha) \\ &\qquad + B_{Arm}(\dot{\theta}_m + \dot{\alpha}) \\ &\qquad = -K_s\alpha \end{aligned} \tag{52}$$

where $\alpha = \theta - \theta_m$ is defined as link deflection and

$$\tau_m = K_1 U_1 - K_2\dot{\theta}_m \tag{53}$$
$$\begin{cases} K_1 = \dfrac{\eta_g K_g \eta_m K_t}{R_m} \\ K_2 = \dfrac{\eta_g K_g^2 \eta_m K_m K_t}{R_m} \end{cases}$$

This can be expressed as follows:

$$\begin{aligned} \ddot{\theta}_m &= \frac{(-K_2 - B_{eq} + B_{Arm})}{J_{eq}}\dot{\theta}_m + \frac{B_{Arm}}{J_{eq}}\dot{\alpha} \\ &\quad + \frac{K_s}{J_{eq}}\alpha + \frac{K_1}{J_{eq}}U_1 \\ \ddot{\alpha} &= \frac{mghsin(\theta_m + \alpha)}{J_{Arm}} \\ &\quad + \left(\frac{K_2 + B_{eq} - B_{Arm}}{J_{eq}} - \frac{B_{Arm}}{J_{Arm}}\right)\dot{\theta}_m \\ &\quad - \frac{B_{Arm}(J_{Arm} + J_{eq})}{J_{Arm}J_{eq}}\dot{\alpha} \\ &\quad - \frac{K_s(J_{Arm} + J_{eq})}{J_{Arm}J_{eq}}\alpha - \frac{K_1}{J_{eq}}U_1 \end{aligned} \tag{54}$$

Taking into account the transformation of the following variables, similar to the explanation provided in the previous section:

$$\begin{aligned} &x_1 = \alpha, x_2 = \theta_m \\ &x_3 = \dot{\alpha}, x_4 = \dot{\theta}_m \end{aligned} \tag{55}$$

Additionally, incorporating $F_a f_a$ as actuator fault, and Δf as unknown dynamics and modeling uncertainties into the robot model in (54), we obtain:

$$\begin{cases} \dot{x}_1 = x_3 \\ \dot{x}_2 = x_4 \\ \dot{x}_3 = f_1 + b_1 U_1 + \Delta f(\theta) \\ \dot{x}_4 = f_2 + b_2 U_1 + F_a f_a \end{cases} \tag{56}$$

where we have:

$$\begin{cases} f_1 = \frac{mghsin(x_1 + x_2)}{J_{Arm}} + \left(\frac{K_2 + B_{eq} - B_{Arm}}{J_{eq}} - \frac{B_{Arm}}{J_{Arm}}\right)x_4 - \frac{B_{Arm}(J_{Arm} + J_{eq})}{J_{Arm}J_{eq}}x_3 - \frac{K_s(J_{Arm} + J_{eq})}{J_{Arm}J_{eq}}x_1 \\ f_2 = \frac{(-K_2 - B_{eq} + B_{Arm})}{J_{eq}}x_4 + \frac{B_{Arm}}{J_{eq}}x_3 + \frac{K_s}{J_{eq}}x_1 \\ b_2 = \frac{K_1}{J_{eq}} \\ b_1 = -\frac{K_1}{J_{eq}} \end{cases} \tag{57}$$

The dynamic parameters of the robot are provided in Table 1. Additionally, we assume the values of the uncertainties and disturbance or faults as follows:

$$\Delta f = 0.5\sin(0.3t) + 0.7sign(x_1) + 2\|\hat{x}\|$$

$$d(t) = \begin{cases} 4 & 4 \le t \le 9 \\ 0 & other \end{cases} \quad (58)$$

It is also worth to mention that in order to address the verification of our mathematical model in this paper, for the flexible joint manipulator (FJM), we conducted a validation procedure, which includes:

Comparison with Existing Literature: We compared our model with established models from previous studies, demonstrating consistency in dynamic behavior and performance metrics.

Simulation Results: Additional simulations using both our state-space model and reference models confirmed the robustness and accuracy of our mathematical representation.

Future Work on Experimental Validation: We acknowledge the importance of experimental validation and plan to implement physical prototyping in future research to further confirm the model's reliability.

The initial conditions are set as $x(0) = [1,2,0,0]^T$ for the angles of the robot and the motor in the robot. All the dynamic parameters of the simulated flexible joint robot are detailed in Table 1. Also, for simulation purposes, the parameters of the controller are chosen as follows, guided by Theorems 1 from the previous sections:

$$\rho = 2, \quad \gamma = 0.7, \quad k = 4\ , \quad \mu = 0.8$$

In order to show the performance of close loop system, a desired sinusoidal path is considered for the flexible joint as a desired trajectory to be tracked. This is done to investigate whether the designed control law can effectively facilitate the sinusoidal movement and reciprocation of the joint angle in a flexible robot.

$$x_{des} = [5\,sin(0.3t) \quad 0 \quad 0 \quad 1.5\cos(0.3t)]^T \quad (59)$$

The simulation results for this scenario are presented in following figures.

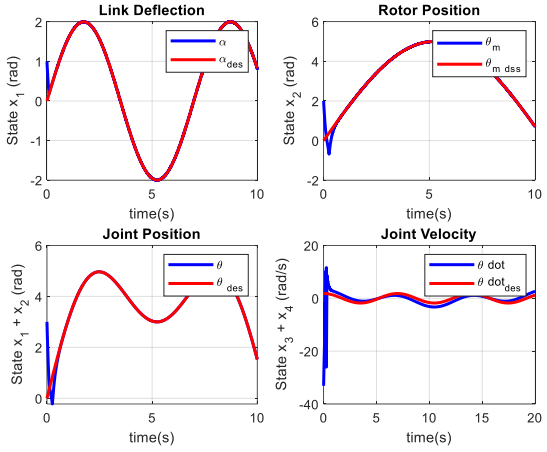

Fig. 1. Convergence of the robot modes to the desired values in simulation

Table.1.
Dynamic parameters of the simulated flexible joint robot [43]

Definition	Parameter	Value
Equivalent Viscous Damping (N.M.S/rad)	B_{Arm}	0.004
Rotor Viscous Friction (N.M.S/rad)	B_{eq}	0.07
Back-EMF Constant (V.S/rad)	K_m	0.00767
Motor Torque Constant (N.M/A)	K_t	0.00767
Total Gear Ratio	K_g	14:5
Gearbox Efficiency	η_g	0.89
Motor Efficiency	η_m	0.84
Motor Resistance (Ω)	R_m	2.4
Joint Stiffness	K_s	1.2485
Equivalent Inertia (kg m^2)	J_{eq}	0.0023
Total Link Inertia (kg m^2)	J_{Arm}	0.00352
Length of the Link (m)	L	0.3
Mass of the Link (kg)	m	0.100
Gravitational Constant (N/m)	g	9.81

Figure 1 illustrates the convergence of the robot system states, specifically, the values of the angles and the derivatives of the angles including rotor position, joint angle, link deflection and joint velocity to the desired values in the regulation mode. Clearly, the designed finite-time sliding mode control law has effectively driven the first two state variables, representing the angles of the joints and the motor, towards fixed values. Simultaneously, the derivatives in the next two angles have converged to their desired values.

The illustrated sliding surfaces in Figure 2 unequivocally demonstrate the anticipated finite-time convergence of the sliding surfaces to zero. Upon closer inspection of the chart, the presence of chattering in the sliding mode becomes apparent. Employing chattering reduction methods proves effective in mitigating this phenomenon. Furthermore, these methods play a crucial role in attenuating disturbances when they occur. Notably, the convergence is discontinuous (non-smooth) at the point of convergence to zero is sliding surfaces, as highlighted in Figure 2.

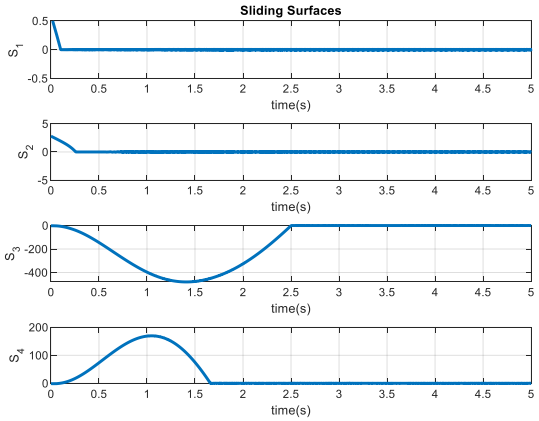

Fig. 2. Sliding surfaces in RAFSMC

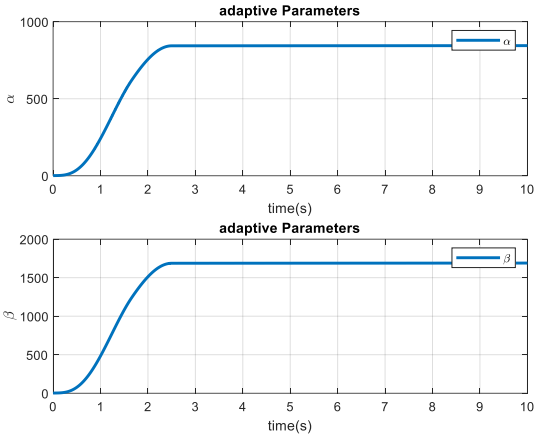

Fig. 3. Adaptive parameters in using ROFOSMC

In the tracking mode, with the convergence of the FJM system states to the desired values, satisfactory results are observed. It is important to note that in such robotic systems, the primary objective is to control the angle of the flexible joint and the angle of the motor, both of which are inherently interconnected. However, as it is clear from figures, all of the robot joint states closely follow the desired sinusoidal values ad their derivatives. In figure 3, the adaptive parameters are shown. According to the Theorem 1, it was expected that given that we have two stable adaptive laws, these two values converge to some bounded fixed values. This is proved in figure 3.

Finally, the input control signal is shown in figure 4. Figure 4 reveals that the input of the system does not reach zero when the states converge to the desired values. This observation aligns with physical principles, as the angles of the robot with flexible joints are required to converge to the sinusoidal signal. Consequently, a continuous control effort along the sinusoidal path is imperative and should not become zero.

As more explanations, in figure 1, unlike in the regulation scenarios, both angles and as a result their derivatives do not converge to zero. In this case, the arm with flexible joints is following a reciprocating and periodic trajectory. As a result, the system is under excitation and unlike the regulation case, it does not reach the equilibrium point. Therefore, we expect energy to be continuously injected into the robot system, which is equivalent to a non-zero input signal, which we also expect to have a periodic and sinusoidal form due to the reciprocating path. An event that is well confirmed by Figure 4.

The most important problem in input control signal in Figure 4 is the chattering phenomena. Therefore, in the next simulations, we can see that using the chattering avoidance idea presented in this paper, the chattering will be decreased cconsiderably. The simulation results in figures 5 to 8, shows the effect of using the chattering avoidance idea presented in this paper.

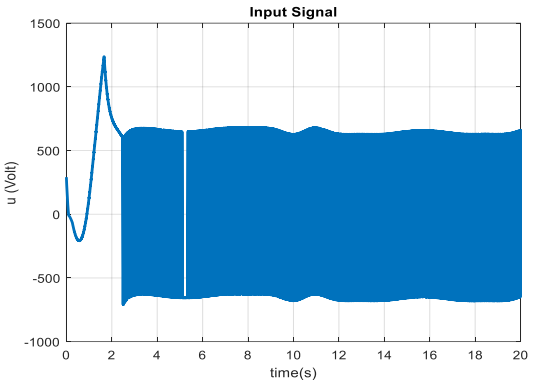

Fig. 4. System input signal

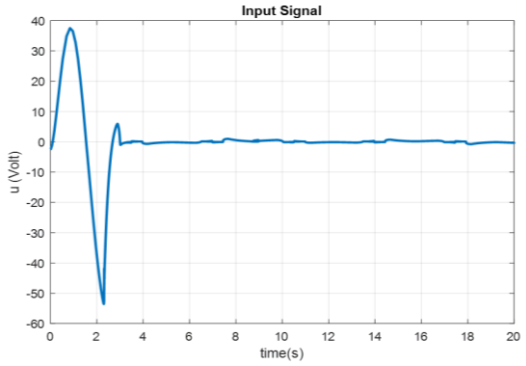

Fig. 5. System input signal using chattering avoidance idea

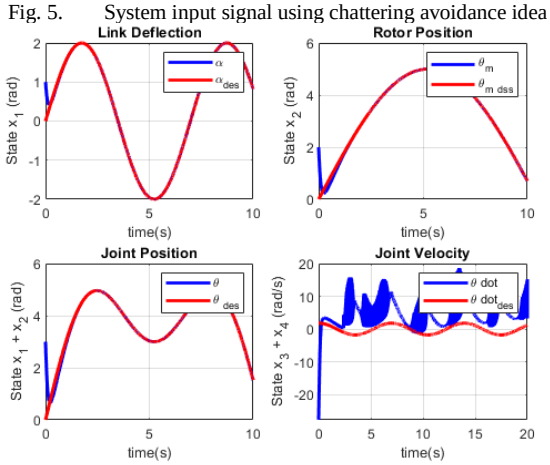

Fig. 6. Convergence of the robot modes to the desired values using chattering avoidance idea

As it is clear from Figure 5, the chattering in the input signal is decreased too much that makes the input control signal to be smoother and therefore realistic and applicable for using in experimental situations. In Figure 6, it is shown that by using the chattering avoidance idea,

It can be seen in Figure 6 that by applying the idea of chattering reduction presented in this article, the convergence of almost all the state variables in the system is achieved well in the same limited time as before. However, the price we have to pay to reduce chattering is the fluctuations in the fourth state variable, i.e. the derivative of the joint's positions meaning joint velocities. This price, of course, is not a big cost because basically the aim in controlling the FJM systems was achieving finite time trajectory tracking in Joint Position and joint velocities are less important.

In Figure 7, the results of convergence of sliding surfaces to zero is shown. Comparing with Figure 2, shows a later convergence of the first two sliding surfaces, although chattering is significantly reduced in return. Finally, if we look at the estimated adaptive parameters in Figure 8, we can see that the result of their convergence to a fixed and limited value is still acceptable, although the final value of their convergence is reduced. The only importance of which is the reduction of the amplitude of the input signal, which is using these parameters as some coefficients. As a result, using the presented RAFSMC control law along with the proposed chattering reduction method provides finite time convergence while eliminating chattering and in the presence of uncertainties, disturbances and faults. This is an important achievement in this field.

A) Sensitivity Analysis of Parameter Uncertainties

To evaluate the robustness of the proposed Robust-Adaptive Finite-Time Sliding Mode Control for Flexible Joint Manipulators, we conducted a comprehensive sensitivity analysis focusing on three dynamic parameters: joint stiffness, mass of the link, and equivalent viscous damping. We applied variations of +20% for joint stiffness, -20% for mass, and +15% for equivalent viscous damping to assess the impact of these parameter uncertainties on performance. Figures 9.a, 9.b, and 9.c collectively illustrate the results of the sensitivity analysis, presenting the rotor position tracking and link deflection against the variations in parameters. The results indicate that, despite minor fluctuations in tracking performance—mostly noticeable in Figure 9.c—the overall stability of the manipulator is preserved throughout the parameter variations. This stability demonstrates the robustness of our control strategy, as both rotor position tracking and link deflection remain largely unaffected by the introduced uncertainties.

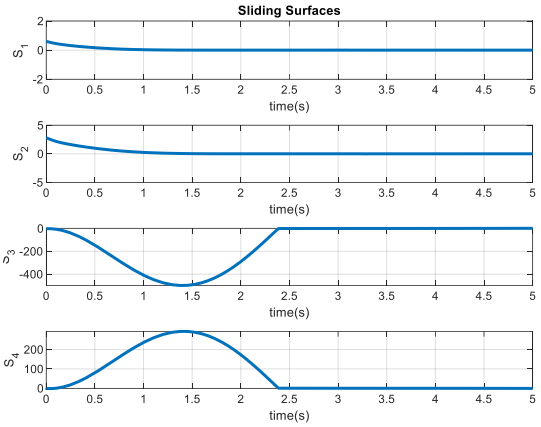

Fig. 7. Sliding surfaces in RAFSMC using chattering avoidance idea

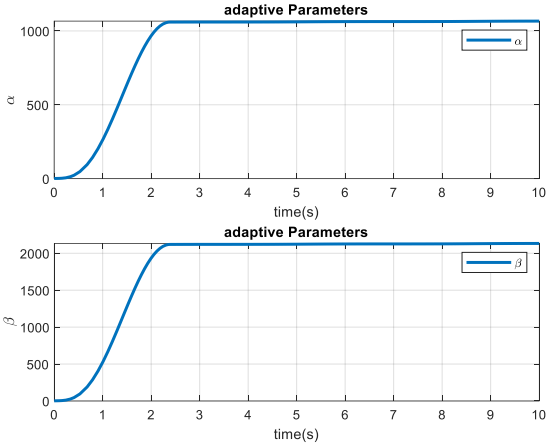

Fig. 8. Adaptive parameters by applying ROFOSMC considering chattering avoidance idea

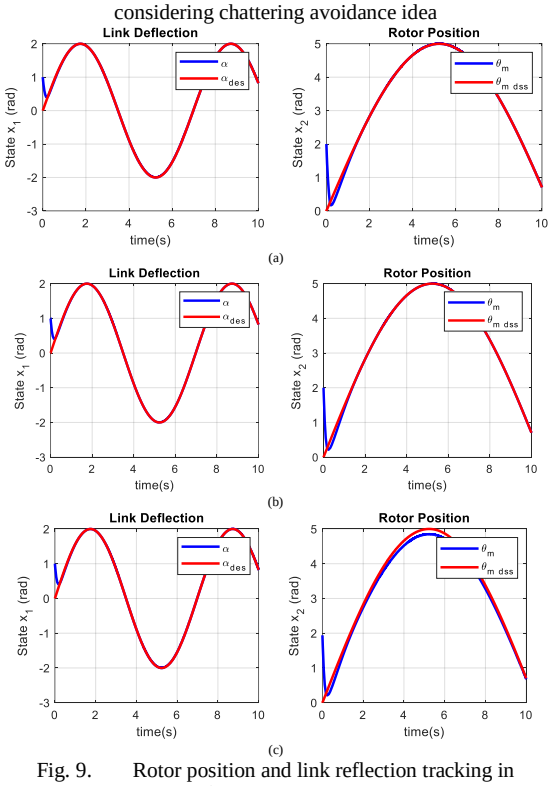

Fig. 9. Rotor position and link reflection tracking in Sensitivity Analysis of dynamic Parameters Uncertainties.a) Variations in joint stiffness. b) Variations in the mass of the link and c) variations in equivalent viscous damping

Table 2 presents the Root Mean Square (RMS) values for the input control signal, rotor tracking error, and link deflection error under varying parameter uncertainties. RMS is a statistical measure that quantifies the magnitude of a varying signal, providing valuable insights into the performance of the control system for a one-link robot manipulator.

Input Control Signal RMS: This value reflects the average power exerted by the controller over the simulation period. Lower RMS values indicate that the controller is using less energy to maintain the desired rotor angle, which is favorable for both efficiency and stability. In our analysis, the RMS values of the input control signal for the three scenarios are approximately 3.2, 2.7, and 2.9, respectively, demonstrating a consistent energy requirement across varying parameter uncertainties.

Tracking Error Signal RMS: This metric quantifies the average deviation of the actual rotor angle from the desired angle over time. Lower RMS values for the tracking error indicate superior tracking performance, signifying that the manipulator closely follows the desired trajectory. In this study, the RMS values for both the rotor tracking error and the link deflection error are notably small and near zero, confirming the effectiveness of the control strategy in maintaining accurate positioning despite the applied uncertainties. Overall, the small RMS values for the rotor tracking error and link deflection error, combined with the moderate RMS values for the input control signal, highlight the robustness and stability of our proposed control approach under varying dynamic conditions.

B) Comparison with other references

In the following, a Comparison with a recent reference paper is presented. To do this, the simulation results obtained in this paper are compared with those obtained from reference [43]. In [43], a robust-adaptive sliding mode control is designed for flexible joint manipulator system in (1)-(2) by considering uncertainties, disturbances and unmodeled dynamic in which first the FJM system is divided to *n* error subsystem and then and for each one a separated sliding surface and SMC controller is designed. The error system of FJM and controller designed in [43] are presented in Table 3.

Considering the fault, uncertainties and unmodeled dynamic as in previous simulation and selecting a regulation scenario for simulation with the following desired point. the simulation results of this comparison are shown in Figure 10, when the control parameters are considered for both controllers same as previous simulation.

$$x_{des} = \begin{bmatrix} 0 & \frac{2\pi}{3} & 0 & 0 \end{bmatrix}^T \quad (60)$$

Table.2.
Root Mean Square (RMS) values under parameter uncertainties

RMS	***Joint stiffness***	***Mass of the link***	***Equivalent viscous damping***
Rotor Tracking error RMS	0.0372	0.0427	0.0594
Link Deflection Tracking error RMS	0.219	0.011	0.199
Input Signal RMS	3.231	2.718	2.947

Table.3.
System and controller designed for stabilizing flexible joint robots in [43]

FJM *n* order error system in [43]	Adaptive SMC method in [43]
$\dot{e}_1 = e_{2n+1},$ $\vdots$ $\dot{e}_n = e_{3n},$ $\dot{e}_{n+1} = e_{3n+1},$ $\vdots$ $\dot{e}_{2n} = e_{4n},$ $\dot{e}_{2n+1} = f_1(e+x_d) + b_1U_1 + d_1(t) - \ddot{x}_{d_1},$ $\vdots$ $\dot{e}_{3n} = f_n(e+x_d) + b_nU_n + d_n(t) - \ddot{x}_{d_n},$ $\dot{e}_{3n+1} = f_{n+1}(e+x_d) + b_{n+1}U_1 + d_{n+1}(t) - \ddot{x}_{d_{n+1}},$ $\vdots$ $\dot{e}_{4n} = f_{2n}(e+x_d) + b_{2n}U_n + d_{2n}(t) - \ddot{x}_{d_{2n}}.$	$U_i = U_{eq_{1_i}} + U_{eq_{2_i}} + U_{sw_i},$ $U_{eq_{1_i}} = -\frac{C_{1_i}e_{2n+i} + f_i(e+x_d) - \ddot{x}_{d_i}}{b_i}.$ $U_{eq_{2_i}} = -\frac{C_{2_i}e_{3n+i} + f_{n+i}(e+x_d) - \ddot{x}_{d_{n+i}}}{b_{n+i}}.$ $U_{sw_i} = -\frac{\gamma_i b_i U_{eq_{2_i}} + b_{n+i}U_{eq_{1_i}} + \lambda_i S_i + \rho_i \operatorname{sgn}(S_i)}{\gamma_i b_i + b_{n+i}}.$

As it is clear from figure 9, the trajectory tracking is not satisfactorily obtained using the method in [43] and for the time in which the disturbance is accrue, both joint and motor position are affected by disturbance and uncertainties.

The comparison shows that when the range of disturbances increases and fault happens, the method presented in [43] did not cope well with the uncertainties, disturbances and fault and the performance of the method presented in the current paper is much better.

This is not the whole issue, the more important point is that in reference [43], it is supposed that the upper bounds of the uncertainties and disturbances must be a scaler fixt bounded and known value for the designer. In [43] there exist this assumption:

$$|d_i| \le D_i, \quad i = 1,2,\dots 2n \quad (61)$$

In addition to that, the condition for proving the stability of the control law presented in [43] in Table 2 is that the parameter ρ_i in the control law is necessary and must be larger than the upper bands of disturbances, i.e.:

$$\rho_i > (\gamma_i D_i + D_{n+i}), \quad i = 1,2,\dots 2n \quad (62)$$

This means that the disturbances upper bounds D_i must be completely known for the designed and should also be scaler fixt and bounded values. The assumptions in (61) for FJM system and (62) for controller are two very conservative conditions that are not exist in our paper and this advantage is much more important than comparisons in Figure 10.

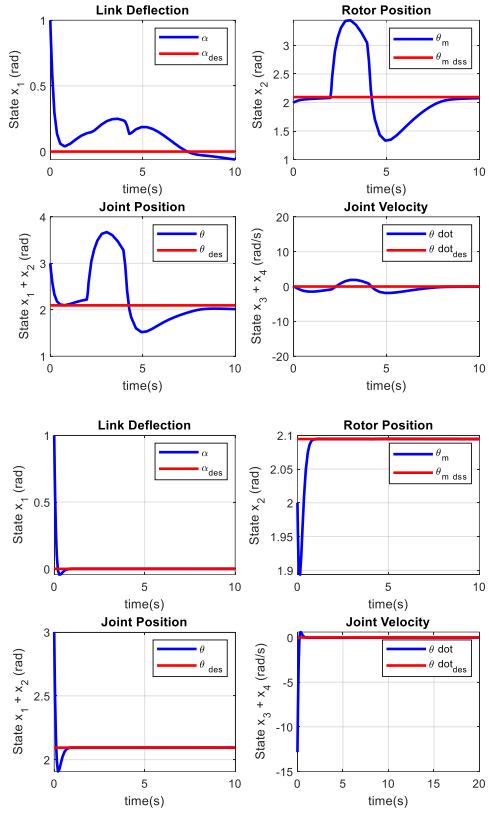

Fig. 10. Comparison of the convergence of the robot modes to the desired values using the RAFSMC method presented in this paper with robust-adaptive SMC method presented in [43].VB-ASMC method proposed in [43] and The RAFSMC method in current paper.

Another very important issue is that, firstly, in reference [43], convergence to the desired values of robot is obtained asymptotically and therefore in infinity time and not finite time. While in the RAFSMC method proposed in current paper, apart from guaranteeing the convergence in a specific finite time, the upper bounds of uncertainties, disturbances and faults is an unknown functional upper bound of system states where the coefficients of this function are estimated via some stable adaptive laws.

At the end of this section, in order to better understand the methodology presented in this paper, the complete control system block diagram proposed in the previous section to achieve finite time convergence in nonlinear model of FJM root is presented in Fiure. 10. The RAFSMC controller block diagram generates the stabilizing finite time control law using: The feedback of the state variables of the flexible manipulator, output of adaptive laws and also sliding surface. In simpler words, the designed controller guarantees finite time stability for flexible joint manipulator in such condition that robot system is exposed to unknown unbounded perturbations with functional upper bund. The coefficients of this functional upper bound that are estimated in adaptive block, are used in input controller as controller parameters.

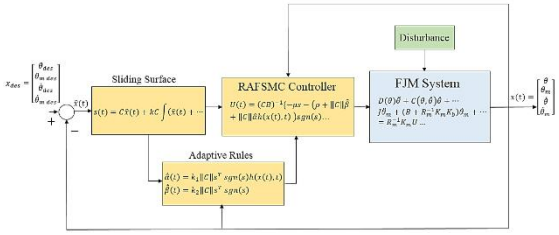

Fig. 11. Fig. 10. The RAFSMC control system block diagram proposed in Section 4

C) *Practical Implications of Simulation Results*

The simulation results presented in this study not only validate the effectiveness of the Robust-Adaptive Finite-Time Sliding Mode Control (RAFSMC) for Flexible Joint Manipulators (FJMs) but also highlight several potential real-world applications. The proposed control strategy can be particularly beneficial in industries where precision and adaptability are crucial, such as robotics, automation, and aerospace engineering.

For instance, in robotic applications, the ability to handle unknown disturbances and uncertainties makes the RAFSMC an ideal candidate for tasks requiring high levels of accuracy and reliability, such as surgical robots or collaborative robots (cobots) working alongside humans. Additionally, the adaptive nature of the controller allows for seamless adjustments to varying operational conditions, thereby enhancing the overall performance of robotic systems in dynamic environments. While we recognize that experimental validation is essential for confirming the real-world applicability of our approach, our simulations have been conducted under conditions that closely resemble practical scenarios. By incorporating unknown disturbances and modeling uncertainties, we aim to ensure that the findings are relevant and applicable to real-world applications. Future work will focus on experimental validation to further substantiate these results.

5. Conclusion

This paper delves into the finite time trajectory tracking in n order flexible joint manipulators by designing a finite time terminal robust adaptive sliding mode control in which the upper bounds of system perturbations including external disturbances, modelling uncertainties and faults is not just a known scaler bounded value, but a nonlinear unknown functional upper bound of FJM states with unknown coefficients that can even be unbounded. To do this, a finite time sliding mode control law is designed using a finite time sliding surface and a RAFSMC method which can provide convergence in a predetermined bounded time in the presence of perturbations and adaptive rules that are used for estimating the perturbations' upper bound

function. The stability proof of whole controller is validated through the application of the Lyapunov method, ensuring stability within a finite period. This control law, operating in the presence of faults and nonlinear components within the flexible joint manipulator system, facilitates the attainment of stability within a constrained timeframe. Ultimately, the simulation results, elucidated through numerical examples, distinctly illustrate the effective functioning of RAFSMC method. At the end of the simulation, the superiority of this method compared to one of the recent references is clearly shown in terms of the problem conditions as well as the convergence of FJM states to their desired values. The proposed RAFSMC approach of this paper can solve the FJM trajectory tracking problem in a more realistic situation when the system is exposed to model uncertainties and external disturbances that are dependent to situation and attitude of a flexible joint manipulator.

References

[1] A Azizi, M Naderi Soorki, T Vedadi Moghaddam, A Soleimanizadeh, A New Fractional-Order Adaptive Sliding-Mode Approach for Fast Finite-Time Control of Human Knee Joint Orthosis with Unknown Dynamic, Mathematics 11 (21), 4511, 2023.

[2] Cong, V.D. Visual servoing control of 4-DOF palletizing robotic arm for vision based sorting robot system.Int. J. Interact. Des. Manuf. (IJIDeM) 2023, 17, 717–728.

[3] Yi, J.B.; Nasrat, S.; Jo, M.S.; Yi, S.J. A Software Platform for Quadruped Robots with Advanced Manipulation Capabilities. Sensors 2023, 23, 8247.

[4] Su, Y.X.; Zheng, C.H. PID control for global finite-time regulation of robot manipulators.Int. J. Syst. Sci. 2017, 48, 547–558.

[5] H. Li, B. Yang, S. Jiang and J. Luo, "Robot Manipulator Trajectory Tracking with Uncertainties Based on Adaptive Sliding Control," 2023 IEEE International Conference on Unmanned Systems (ICUS), Hefei, China, 2023, pp. 1434-1439, 2023.

[6] M. Zhang, Z. Zhang and M. Sun, "Adaptive Tracking Control of Uncertain Robotic Manipulators," in IEEE Transactions on Circuits and Systems II: Express Briefs, vol. 71, no. 5, pp. 2734-2738, May 2024.

[7] K. Dileep, S. J. Mija and N. K. Arun, "Radial Basis Function Neural Network Based PID Tuning for Trajectory Tracking in Robot Manipulator," 2024 15th International Conference on Computing Communication and Networking Technologies (ICCCNT), Kamand, India, 2024, pp. 1-7.

[8] B. Li, X. Li, H. Gao and F. -Y. Wang, "Advances in Flexible Robotic Manipulator Systems — Part II: Planning, Control, Applications, and Perspectives," in IEEE/ASME Transactions on Mechatronics, vol. 29, no. 3, pp. 1680-1689, June 2024

[9] H. Wang, Y. Zhang, Z. Zhao, X. Tang, J. Yang, I.-M. Chen, Finite-time disturbance observer-based trajectory tracking control for flexible-joint robots, Nonlinear Dynamics 106 (1) (2021) 459–471.

[10] K. Li, H. Zhang and H. Wang, "Nonlinear Observer-Based Visual Servoing and Vibration Control of Flexible Robotic Manipulators With a Fixed Camera," in IEEE Transactions on Cybernetics, vol. 54, no. 7, pp. 4100-4110, July 2024.

[11] B. Zhan, M. Jin, J.Liu, "Extended-state-observer-based adaptive control of flexible-joint space manipulators with system uncertainties," Advances in Space Research, Vol. 69, no. 8, pp. 3088-3102, 2022.

[12] W. Chang, Y. Li and S. Tong, "Adaptive Fuzzy Backstepping Tracking Control for Flexible Robotic Manipulator," in IEEE/CAA Journal of Automatica Sinica, vol. 8, no. 12, pp. 1923-1930, December 2021.

[13] W. Sun, S.-F. Su, J. Xia, V.-T. Nguyen, Adaptive fuzzy tracking control of flexible-joint robots with full-state constraints, IEEE transactions on Systems, Man, and Cybernetics: Systems 49 (11) (2018) 2201–2209.

[14] H. Gao, W. He, C. Zhou, C. Sun, Neural network control of a two-link flexible robotic manipulator using assumed mode method, IEEE Transactions on Industrial Informatics 15 (2) (2018) 755–765.

[15] Y. Pan, X. Li, H. Yu, Efficient pid tracking control of robotic manipulators driven by compliant actuators, IEEE Transactions on Control Systems Technology 27 (2) (2019) 915–922.

[16] Ak, A. Sliding Mode Controller Design Using Fuzzy Sliding Surface for Flexible Joint Manipulator. IETE Journal of Research, 68(1), 760–767. 2021.

[17] Gao Y, Lu H. Sliding Mode Control of Flexible Articulated Manipulator Based on Robust Observer. Jan 4, 2440770. Retraction in: Computer Intelligent Neuroscience. 2022.

[18] Azeez, M.I., Abdelhaleem, A.M.M., Elnaggar, S. et al. Optimized sliding mode controller for trajectory tracking of flexible joints three-link manipulator with noise in input and output. Sci Rep 13, 12518, 2023.

[19] Majidi B., Ikbel B. CH. A., Zie H., sliding mode controller design: stability analysis and tracking control for flexible joint manipulator. rrst-ee. 2021;66(3):161-167. Accessed August 17, 2024.

[20] Shixuan Zhang, Wan-Cheng Wang, Adaptive sliding mode robust control of manipulator driven by tendon-sheath based on HJI theory, Measurement and Control, 55, 684 – 702, 2022.

[21] Kamal Rsetam, Mohammad Al-Rawi, Zhenwei Cao, Zhihong Man, Sliding mode control based on high-order extended state observer for flexible joint robot under time-varying disturbance, AIP Conf. Proc. 2651, 05001, 2023.

[22] Cheng, X.; Liu, H.; Lu, W. Chattering-Suppressed Sliding Mode Control for Flexible-Joint Robot Manipulators. Actuators 2021, 10, 288, 2021.

[23] S. zaare, M. R. Soltanpour, M. Moattari," Voltage based sliding mode control of flexible joint robot manipulators in presence of uncertainties," Robotics and Autonomous Systems, vol. 118, pp. 204-219, 2019.

[24] K. Rsetam, Z. Cao, Z. Man, M. Mitrevska, Optimal second order integral sliding mode control for a flex-ible joint robot manipulator, in: IECON 2017-43rd Annual Conference of the IEEE Industrial Electronics Society, IEEE, 2017, pp. 3069–3074, 2017.

[25] H. Du, G. Wen, Y. Cheng, W. Lu, T. Huang, Designing discrete-time sliding mode controller with mis-matched disturbances compensation, IEEE Transactions on Industrial Informatics 16 (6), 4109–4118, 2019.

[26] A.-C. Huang, Y.-C. Chen, Adaptive sliding control for single-link flexible-joint robot with mismatched un-certainties, IEEE Transactions on Control Systems Technology 12 (5), 770–775, 2004.

[27] K. A. Rsetam, Z. Cao, Z. Man, Cascaded extended state observer based sliding mode control for underactu-ated flexible joint robot, IEEE Transactions on Industrial Electronics, 2019.

[28] S. Chávez-Vázquez, J. E. Lavín-Delgado, J. F. Gómez-Aguilar, J. R. Razo-Hernández, S. Etemad, S. Rezapour, "Trajectory tracking of Stanford robot manipulator by fractional-order sliding mode control," Applied Mathematical Modelling, Vol. 120, pp. 436-462, 2023

[29] Z. Yan, X. Lai, Q. Meng, J. She, M. Wu, "Time-varying disturbance-observer-based tracking control of uncertain flexible-joint manipulator," Control Engineering Practice, Vol. 139, pp. 105624, 2023.

[30] L. Liu, W. Yao, Y. Guo, "Prescribed performance tracking control of a free-flying flexible-joint space robot with disturbances under input saturation," Journal of the Franklin Institute, Vol. 358, no. 9, pp. 4571-4601, 2021.

[31] M. Ramírez-Neria, G. Ochoa-Ortega, N. Lozada-Castillo, M. A. Trujano-Cabrera, J. P. Campos-López, and A. Luviano-Juárez, ``On the robust trajectory tracking task for flexible-joint robotic arm with unmodeled dynamics," IEEE Access, vol. 4, pp. 7816_7827, 2016.
[32] D. Shang, X. Li, M. Yin, F. Li,"Dynamic modeling and fuzzy adaptive control strategy for space flexible robotic arm considering joint flexibility based on improved sliding mode controller," Advances in Space Research, Vol. 70, no. 11, pp. 3520-3539, 2022.
[33] S. Zhang, Y. Wu, X. He and J. Wang, "Neural Network-Based Cooperative Trajectory Tracking Control for a Mobile Dual Flexible Manipulator," in IEEE Transactions on Neural Networks and Learning Systems, vol. 34, no. 9, pp. 6545-6556, Sept. 2023.
[34] K. Rsetam, Z. Cao and Z. Man, Design of Robust Terminal Sliding Mode Control for Underactuated Flexible Joint Robot," in IEEE Transactions on Systems, Man, and Cybernetics: Systems, vol. 52, no. 7, pp. 4272-4285, July 2022,
[35] M. Hong, X. Gu, L. Liu, Y. Guo, "Finite time extended state observer based nonsingular fast terminal sliding mode control of flexible-joint manipulators with unknown disturbance," Journal of the Franklin Institute, vol. 360, no. 1, pp.18-37, 2023.
[36] Jing C, Zhang H, Liu Y, Zhang J. Adaptive Super-Twisting Sliding Mode Control for Robot Manipulators with Input Saturation. Sensors. 2024; 24(9), 2783, 2024.
[37] J. Moyrón, J. Moreno-Valenzuela and J. Sandoval, "Global Regulation of Flexible Joint Robots With Input Saturation by Nonlinear I-PID-Type Control," in IEEE Transactions on Control Systems Technology, vol. 32, no. 6, pp. 2385-2393, Nov. 2024.
[38] J. Wang, X. Yan and L. Yu, "Enhanced Friction and Disturbance Compensation-Based Trajectory Tracking Control for Flexible Manipulator System," in IEEE Journal of Emerging and Selected Topics in Industrial Electronics, vol. 5, no. 3, pp. 1322-1332, July 2024.
[39] R. F. A. Khan, K. Rsetam, Z. Cao and Z. Man, "Singular Perturbation-Based Adaptive Integral Sliding Mode Control for Flexible Joint Robots," in IEEE Transactions on Industrial Electronics, vol. 70, no. 10, pp. 10516-10525, Oct. 2023.
[40] N. X. Chiem, T. X. Pham, P. D. Thai and T. C. Phan, "An Adaptive Sliding-mode Controller for Flexible-joint Manipulator," 2023 12th International Conference on Control, Automation and Information Sciences (ICCAIS), Hanoi, Vietnam, 2023.
[41] Khooban, M.H., Niknam, T., Blaabjerg, F., Dehghani,M.: Free chattering hybrid sliding mode control for a class of non-linear systems: electric vehicles as a case study. IET Sci. Meas. Technol. Vol. 10, no. 7, pp. 776–785, 2016.
[42] Shokoohinia, M.R., Fateh, M.M.: Robust dynamic sliding mode control of robot manipulators using the Fourier series expansion. Trans. Inst. Meas. Control 1–8, 2018.
[43] S. Zaare, S., Soltanpour, M. R., Moattari, Adaptive sliding mode control of n flexible-joint robot manipulators in the presence of structured and unstructured uncertainties," Multibody System Dynamics 47, pp. 397-434, 2019.